V European Conference on Computational Fluid Dynamics
ECCOMAS CFD 2010
J. C. F. Pereira and A. Sequeira (Eds)
Lisbon, Portugal,14-17 June 2010

ON RESTRAINING SUBGRID-SCALE PRODUCTION IN BURGERS' EQUATION

Joop A. Helder[*,†] **and Roel W.C.P. Verstappen**[†]

[†] Institute of Mathematics and Computing Science, University of Groningen,
P.O.Box 800, 9700AV Groningen, The Netherlands
e-mail: j.a.helder@rug.nl, r.w.c.p.verstappen@rug.nl

[*] MARIN Maritime Research Institute Netherlands,
P.O.Box 28, 6700AA Wageningen, The Netherlands
email: j.a.helder@marin.nl

Key words: Turbulence modeling, Regularization, Large-eddy simulation, Burgers' equation, Vortex stretching, Subgrid-scale restrainment

Abstract. *Most turbulent flows cannot be computed directly from the incompressible Navier-Stokes equations, because the convective term produces too many scales of motion. In the quest for a dynamically less complex mathematical formulation, we consider regularizations of the nonlinearity. The obtained regularized system is more amenable to approximate numerically, while its solution approximates the dynamically relevant part of the Navier-Stokes solution. Hereby, we propose to preserve the symmetry and conservation properties of the original convective term. The underlying idea is to restrain the convective production of small scales in an unconditionally stable manner, meaning that the regularized solution can not blow up in the energy norm. By analysing the regularized triad interactions in detail, a filter length is determined dynamically, such that the vortex-stretching process stops (approximately) at the grid-scale, all through the domain, at all times. This constitutes a parameter-free regularization model which converges to the Navier-Stokes solution when grid resolution is sufficiently high. In this paper, as a first step, the regularization model is tested for Burgers' equation. This makes a more detailed analysis possible, while important aspects of the Navier-Stokes equations remain. Energy spectra follow DNS results for the large scale motions, whereas a much steeper power law is found for small scales, which is precisely what a regularization model is ought to do.*

1 INTRODUCTION

It is generally accepted that the Navier-Stokes equations provide an appropriate model for the nonlinear dynamics of turbulence. For an incompressible flow, the equations are

$$\partial_t \boldsymbol{u} + \mathcal{C}(\boldsymbol{u}, \boldsymbol{u}) = -\nabla p + \mathcal{D}(\boldsymbol{u}), \tag{1}$$

where $\boldsymbol{u}$ denotes the fluid velocity, and p represents the pressure. The dissipative term is given by $\mathcal{D}(\boldsymbol{u}) = \Delta \boldsymbol{u}/\mathrm{Re}$, where Re denotes the Reynolds number, and the nonlinear, convective term is defined by $\mathcal{C}(\boldsymbol{u}, \boldsymbol{v}) = (\boldsymbol{u} \cdot \nabla)\boldsymbol{v}$. Attempts at solving turbulent flows directly from the Navier-Stokes equations fail for high Reynolds numbers, because the number of dynamically relevant scales of motion becomes too large. The computationally almost numberless small scales result from the convective term that allows for the transfer of energy from the large scales at which the flow is driven to the smallest scales that can survive viscous dissipation. At the present level of computing power and numerical algorithms, it is not yet possible to calculate the full energy cascade, i.e. all degrees of freedom incorporated in a high Reynolds turbulent flow, see e.g. [1].
In quest of a dynamically less complex mathematical formulation, approximate models have been devised for representing the interaction between the almost uncomputable small scales and the larger ones. In large-eddy simulation (LES), this it done by applying a spatial filter to the Navier-Stokes equations:

$$\partial_t \overline{\boldsymbol{u}} + \mathcal{C}(\overline{\boldsymbol{u}}, \overline{\boldsymbol{u}}) = -\nabla p + \mathcal{D}(\overline{\boldsymbol{u}}) + \mathrm{model}(\overline{\boldsymbol{u}}), \tag{2}$$

where the filtered (read: large-scale) velocity is denoted by $\overline{\boldsymbol{u}}$. The subgrid-scale or closure model in the right-hand side of (2) models the commutator of $\mathcal{C}$ and the filter, *i.e.* $\mathrm{model}(\overline{\boldsymbol{u}}) \approx \mathcal{C}(\overline{\boldsymbol{u}}, \overline{\boldsymbol{u}}) - \overline{\mathcal{C}(\boldsymbol{u}, \boldsymbol{u})}$. Appropriate closure models are hard to find for a number of reasons, see e.g. [2]. A significant reduction of the computational complexity is not to be expected unless the spectral support of the solution is reduced, indicating the requirement of an *inexact* closure. In practice, closure models are often based on phenomenological arguments and mathematically unjustifiable assumptions. Today, a large number of models exist, see [4] and the references therein.
In this paper, regularization is considered as a mechanism to reduce the complexity of the dynamics [2], [3]. More specifically, we propose to regularize the convective term in the Navier-Stokes equations directly:

$$\partial_t \boldsymbol{u} + \widetilde{\mathcal{C}}(\boldsymbol{u}, \boldsymbol{u}) = -\nabla p + \mathcal{D}(\boldsymbol{u}). \tag{3}$$

The above regularized system should be more amenable to approximate numerically, while its solution has to approximate the large-scale dynamical behavior of the Navier-Stokes solution. The first outstanding result in this direction goes back to Leray [5], who took $\widetilde{\mathcal{C}}(\boldsymbol{u}, \boldsymbol{u}) = \mathcal{C}(\overline{\boldsymbol{u}}, \boldsymbol{u})$, and proved that a moderate filtering of the transport velocity is sufficient to regularize a turbulent flow. Another example that falls into this concept is

the Navier-Stokes-alpha model [6].
The regularization method basically alters the nonlinearity to restrain the production of small scales of motion. In doing so, one can preserve certain fundamental properties of the convective operator in the Navier-Stokes equations exactly. We propose to preserve the symmetry properties that form the basis for the conservation of energy, enstrophy (in 2D) and helicity (see [7] for details):

$$(\mathcal{C}(\boldsymbol{u},\boldsymbol{v}),\boldsymbol{w}) = -(\mathcal{C}(\boldsymbol{u},\boldsymbol{w}),\boldsymbol{v}), \tag{4a}$$

$$(\mathcal{C}(\boldsymbol{u},\boldsymbol{v}),\Delta\boldsymbol{v}) = (\mathcal{C}(\Delta\boldsymbol{v},\boldsymbol{v}),\boldsymbol{u}), \tag{4b}$$

where the second equality holds only in 2D, and the brackets denote the usual scalar product, i.e $(\boldsymbol{u},\boldsymbol{v}) = \int_\Omega \boldsymbol{u}\cdot\boldsymbol{v}d\boldsymbol{x}$. This criterion yields a class of approximations $\widetilde{\mathcal{C}}(\boldsymbol{u},\boldsymbol{v}) = \mathcal{C}_n(\boldsymbol{u},\boldsymbol{v})$, with

$$\mathcal{C}_2(\boldsymbol{u},\boldsymbol{v}) = \overline{\mathcal{C}(\overline{\boldsymbol{u}},\overline{\boldsymbol{v}})}, \tag{5}$$

$$\mathcal{C}_4(\boldsymbol{u},\boldsymbol{v}) = \mathcal{C}(\overline{\boldsymbol{u}},\overline{\boldsymbol{v}}) + \overline{\mathcal{C}(\boldsymbol{u}',\overline{\boldsymbol{v}})} + \overline{\mathcal{C}(\overline{\boldsymbol{u}},\boldsymbol{v}')} \tag{6}$$

$$\mathcal{C}_6(\boldsymbol{u},\boldsymbol{v}) = \mathcal{C}(\overline{\boldsymbol{u}},\overline{\boldsymbol{v}}) + \mathcal{C}(\boldsymbol{u}',\overline{\boldsymbol{v}}) + \mathcal{C}(\overline{\boldsymbol{u}},\boldsymbol{v}') + \overline{\mathcal{C}(\boldsymbol{u}',\boldsymbol{v}')}, \tag{7}$$

see [8]. Here, the filter operator is again denoted by a bar, and a prime is used to indicate the residual, that is $\boldsymbol{u}' = \boldsymbol{u} - \overline{\boldsymbol{u}}$. Since properties (4) form the basis for the conservation of energy, enstrophy (in 2D) and helicity, and the approximations $\mathcal{C}_n(\boldsymbol{u},\boldsymbol{v})$ inherit these properties by construction, the regularizations are intrinsically stable. For a symmetric filter, the difference between the approximation $\mathcal{C}_n$ and $\mathcal{C}$ is of the order ϵ^n (with $n = 2, 4, 6$), where ϵ denotes the length of the filter. The Leray model and NSα-model are of the order ϵ^2.
The evolution of the vorticity $\boldsymbol{\omega} = \nabla\times\boldsymbol{u}$ resembles that of the Navier-Stokes equations:

$$\partial_t\boldsymbol{\omega} + \mathcal{C}_n(\boldsymbol{u},\boldsymbol{\omega}) + \mathcal{D}(\boldsymbol{\omega}) = \mathcal{C}_n(\boldsymbol{\omega},\boldsymbol{u}). \tag{8}$$

The only difference is that $\mathcal{C}$ is replaced by the regularization $\mathcal{C}_n$. The regularization counteracts the production of small scales of motion by means of vortex stretching, while ensuring stability (in the energy-norm). By analyzing the regularized triad interactions in detail, the filter length can be determined such that the vortex stretching process stops (approximately) at the grid-scale.
In this paper, the approximation $\mathcal{C}_4$ is applied to Burgers' equation in one spatial dimension. This makes a more detailed analysis possible, while important aspects of the Navier-Stokes equations remain. A spectral approach is followed, yet other solution methods may also be used.

2 BURGERS' EQUATION

In the notation of the previous section, the Burgers equation becomes

$$\partial_t u + \mathcal{C}(u,u) = \mathcal{D}(u), \tag{9}$$

where the convective term and the diffusive term are now given by $\mathcal{C}(u,v) = u\partial_x v$ and $\mathcal{D}(u) = \partial^2_{xx} u/\mathrm{Re}$. We consider Equation (9) on an interval Ω with periodic boundary conditions.
In Fourier space, the Burgers equation reads

$$\partial_t \hat{u}_k + \mathcal{C}_k(\hat{u},\hat{u}) = -(k^2/\mathrm{Re})\hat{u}_k + F_k, \tag{10}$$

where the forcing term is given by $F_k \equiv 0$ for $k > 1$ and F_1 such that $\partial_t \hat{u}_1 = 0$ for all t. Here, $\hat{u}_k(t)$ denotes the k-th Fourier coefficient of $u(x,t)$ and the nonlinear term consists of all interactions between modes $\hat{u}_p$ and $\hat{u}_q$ with $p+q=k$, i.e. $\mathcal{C}_k(\hat{u},\hat{u}) = \sum_{p+q=k} \hat{u}_p \mathrm{i}q\hat{u}_q$. The energy e_k of mode k is obtained by taking the product of $\hat{u}_k$ with its complex conjugate $\hat{u}^*_k$, and the evolution of e_k (without forcing) reads

$$\partial_t e_k = -(2k^2/\mathrm{Re})e_k - \hat{u}_k \mathcal{C}_k(\hat{u},\hat{u})^* - \hat{u}^*_k \mathcal{C}_k(\hat{u},\hat{u}). \tag{11}$$

3 SYMMETRY AND CONSERVATION PROPERTIES

In three spatial dimensions, the convective contribution cancels from the energy equation due to the skew-symmetry of the trilinear form $(\mathcal{C}(\boldsymbol{u},\boldsymbol{v}),\boldsymbol{w})$. Indeed, differentiating $(\boldsymbol{u},\boldsymbol{u})$ with respect to time and rewriting $\partial_t \boldsymbol{u}$ with the help of Equation (1) results in a convective contribution of $(\mathcal{C}(\boldsymbol{u},\boldsymbol{u}),\boldsymbol{u})$, which according to Equation (4a) vanishes. As a result, the enstrophy $|\boldsymbol{\omega}|^2$ determines the rate of dissipation of the energy through

$$\partial_t \tfrac{1}{2}|\boldsymbol{u}|^2 = -\tfrac{1}{\mathrm{Re}}|\boldsymbol{\omega}|^2.$$

Furthermore, the evolution of the enstrophy is governed by $\partial_t \frac{1}{2}|\boldsymbol{\omega}|^2 = (\boldsymbol{\omega}, \mathcal{D}(\boldsymbol{\omega}) + \mathcal{C}(\boldsymbol{\omega},\boldsymbol{u}))$. For Burgers' equation, the evolution of the energy $(u,u) = \int_\Omega u^2 dx$ is obtained by following the same steps, resulting in

$$\partial_t \tfrac{1}{2}|u|^2 = -\tfrac{1}{\mathrm{Re}}|\partial_x u|^2.$$

Hence in one spatial dimension, $|\partial_x u|^2$ determines the rate of dissipation of the energy. As in 3D, the convective contribution has vanished, now through $(\mathcal{C}(u,u),u) = \int_\Omega u^2 \partial_x u dx = \frac{1}{3}u^3|_{\partial\Omega} = 0$. The time-rate change of $|\partial_x u|^2$ is given by $\frac{\partial}{\partial t}\frac{1}{2}|\partial_x u|^2 = (\partial_x u, \mathcal{D}(\partial_x u) - \frac{1}{2}\mathcal{C}(\partial_x u, u))$ and resembles that of the 3D enstrophy, differing only a factor $-\frac{1}{2}$ in the second term on the right.

4 SUBGRID-SCALE PRODUCTION

In three spatial dimensions, the production of smaller vortical structures is intimately tied up with the intensification of the vorticity vector $\boldsymbol{\omega}$. A positive convective contribution on the right-hand side of (8) may cause a local increase of the vorticity magnitude, implying that fluid elements are being stretched. This phenomenon, called *vortex stretching*, is responsible for the transfer of energy to smaller an smaller scales of motion.
In a numerical simulation, the production of smaller scales should stop at the smallest

scale that can be represented correctly on the computational grid. On a 1D uniform grid with spacing h, the smallest scale is characterized by the cut-off wavenumber $k_\mathrm{c} = \pi/h$. Inspired by the previous section, we propose to consider $\partial_x u$ for analyzing the process responsible for the small-scale production in one spatial dimension. The time evolution of the spatial derivative of u is governed by

$$\partial_t(\partial_x u) + \mathcal{C}(u, \partial_x u) + \mathcal{D}(\partial_x u) = -\mathcal{C}(\partial_x u, u), \tag{12}$$

which strongly resembles the evolution of $\boldsymbol{\omega}$ given by equation (8), differing only a sign in the term on the right. The k-th Fourier mode of $\partial_x u$ has coefficient $ik\hat{u}_k$. If this coefficient is magnified (i.e. $k^2\hat{u}_k\hat{u}_k^*$ increases), a smaller scale is produced since the increase in slope leads to a steepened up velocity profile. If the mode under consideration has wavenumber k_c, a magnification of $ik_\mathrm{c}\hat{u}_{k_\mathrm{c}}$ produces a mode that cannot be represented correctly on the computational grid, since it has a wavenumber larger than k_c. Hence in 1D, a magnification of $ik_\mathrm{c}\hat{u}_{k_\mathrm{c}}$ introduces numerical error (see Fig. 1).

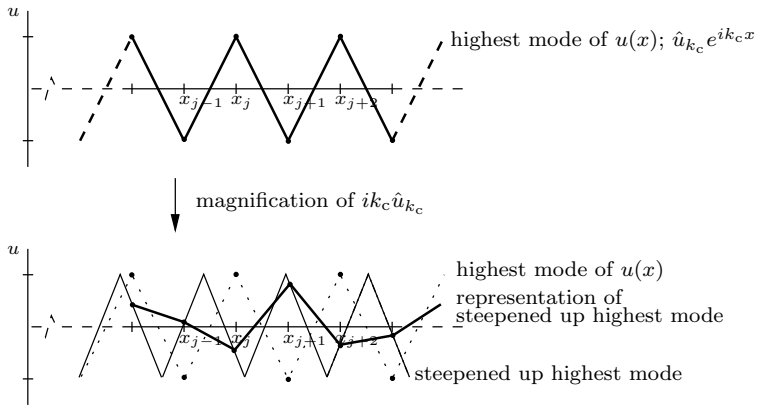

Figure 1: *The highest mode of the velocity that can be represented correctly on the computational grid (above) produces a steepened up profile (below), and introduces numerical error.*

Motivated by this 1D-3D parallel in production of small scales we denote $\omega \overset{\text{def}}{=} \partial_x u$. Its Fourier modes have coefficients $\hat{\omega}_k = \mathrm{i}k\hat{u}_k$, and the evolution of its magnitude $\hat{\omega}_k\hat{\omega}_k^*$ at the smallest grid scale is given by

$$\partial_t(\hat{\omega}_{k_\mathrm{c}}\hat{\omega}_{k_\mathrm{c}}^*) = -(2k_\mathrm{c}^2/\mathrm{Re})\hat{\omega}_{k_\mathrm{c}}\hat{\omega}_{k_\mathrm{c}}^* - \mathrm{i}k_\mathrm{c}\big(\hat{\omega}_{k_\mathrm{c}}^*\mathcal{C}_{k_\mathrm{c}}(\hat{u},\hat{u}) - \hat{\omega}_{k_\mathrm{c}}\mathcal{C}_{k_\mathrm{c}}(\hat{u},\hat{u})^*\big), \tag{13}$$

where again k_c denotes the cut-off wavenumber of the numerical solution, and a superscript $*$ denotes complex conjugate. No magnification of $ik_\mathrm{c}\hat{u}_{k_\mathrm{c}}$ requires that $\partial_t(\hat{\omega}_{k_\mathrm{c}}\hat{\omega}_{k_\mathrm{c}}^*) \leq 0$. Since the diffusive contribution $-(2k_\mathrm{c}^2/\mathrm{Re})\hat{\omega}_{k_\mathrm{c}}\hat{\omega}_{k_\mathrm{c}}^*$ is negative, this condition reads

$$c \leq 0 \quad \text{or} \quad c \geq 1 \qquad \text{with} \quad c \overset{\text{def}}{=} \frac{2\mathrm{i}k_\mathrm{c}\hat{\omega}_{k_\mathrm{c}}\hat{\omega}_{k_\mathrm{c}}^*}{(\hat{\omega}_{k_\mathrm{c}}^*\mathcal{C}_{k_\mathrm{c}}(\hat{u},\hat{u}) - \hat{\omega}_{k_\mathrm{c}}\mathcal{C}_{k_\mathrm{c}}(\hat{u},\hat{u})^*)\mathrm{Re}}. \tag{14}$$

Note that this condition is necessary to stop the highest-frequency mode from producing subgrid scales. To what extend the possible energy flow from lower-frequency modes to subgrid scales (due to strongly nonlinear interactions) is restrained, will become clear from the results.

5 RESTRAINING METHOD

If Condition (14) is satisfied, no scales of motion smaller than the meshsize are produced by the convective term, and Equation (10) can be solved directly. However, when this condition is not satisfied, the convective production of subgrid scales has to be restrained. To that end, we consider the approximation given by Equation (6). In the spectral space the convective term is then approximated by

$$\mathcal{C}_{4,k}(\hat{u},\hat{v}) = \sum_{p+q=k} f(\widehat{G}_k,\widehat{G}_p,\widehat{G}_q) \quad \hat{u}_p \mathrm{i} q \hat{v}_q, \tag{15}$$

where $\widehat{G}_k$ denotes the Fourier transform of the kernel of the convolution filter and

$$f(\widehat{G}_k,\widehat{G}_p,\widehat{G}_q) = \widehat{G}_k(\widehat{G}_p+\widehat{G}_q) + \widehat{G}_p\widehat{G}_q(1-2\widehat{G}_k) \tag{16}$$

This function satisfies $f(1,1,1)=1$ and $f(0,0,0)=0$. Furthermore, all the first-order partial derivatives of $f(\widehat{G}_k,\widehat{G}_p,\widehat{G}_q)$ are strictly positive for $0<\widehat{G}_k,\widehat{G}_p,\widehat{G}_q<1$. Hence, the factor $f(\widehat{G}_k,\widehat{G}_p,\widehat{G}_q)$ by which every nonlinear interaction is reduced is a monotone function of $\widehat{G}_k$, $\widehat{G}_p$, and $\widehat{G}_q$.

In general, the value of the reduction factor $f(\widehat{G}_k,\widehat{G}_p,\widehat{G}_q)$ depends on p and q; hence the terms in the summation in the right-hand side of (15) are damped differently. To avoid this, a discrete 5-points filter in physical space is constructed such that for $k=k_\mathrm{c}$ the function $f(\widehat{G}_{k_\mathrm{c}},\widehat{G}_p,\widehat{G}_q)$ is almost independent of p and q. Then,

$$\mathcal{C}_{4,k_\mathrm{c}}(\hat{u},\hat{v}) \approx \tilde{f}(\widehat{G}_{k_\mathrm{c}})\ \mathcal{C}_{k_\mathrm{c}}(\hat{u},\hat{v}),$$

and the value of the function $\tilde{f}(\widehat{G}_{k_\mathrm{c}})$ follows from Condition (14) with $\mathcal{C}_{k_\mathrm{c}}$ replaced by $\mathcal{C}_{4,k_\mathrm{c}}$:

$$\tilde{f}(\widehat{G}_{k_\mathrm{c}}) = \frac{2\mathrm{i}k_\mathrm{c}\hat{\omega}_{k_\mathrm{c}}\hat{\omega}^*_{k_\mathrm{c}}}{(\hat{\omega}^*_{k_\mathrm{c}}\mathcal{C}_{k_\mathrm{c}}(\hat{u},\hat{u}) - \hat{\omega}_{k_\mathrm{c}}\mathcal{C}_{k_\mathrm{c}}(\hat{u},\hat{u})^*)\mathrm{Re}}. \tag{17}$$

Note that (i) the right-hand side of (17) equals c, and (ii) the same condition can also be derived from the energy equation, since $\hat{\omega}_k\hat{\omega}^*_k = k^2\hat{u}_k\hat{u}^*_k$. With the help of this relation, the equation for $\hat{\omega}_k\hat{\omega}^*_k$ can be easily transferred into the energy equation, and vice versa. We continue by considering the energy: if the Burgers equation is integrated in time with the help of the forward Euler scheme, the discrete time evolution of the energy is given by

$$\frac{[\hat{u}_k]^{n+1}[\hat{u}^*_k]^{n+1} - [\hat{u}_k]^n[\hat{u}^*_k]^n}{\delta t} = [\hat{u}^*_k]^n[W_k]^n + [\hat{u}]^n_k[W^*_k]^n + \delta t[W_k]^n[W^*_k]^n, \tag{18}$$

where an n and $n+1$ denote the old and new time-level respectively, $W_k \stackrel{\text{def}}{=} -\mathcal{C}_{4,k}(\hat{u},\hat{u}) - (k^2/\mathrm{Re})\hat{u}_k$, and δt denotes the time step. The last term in the right-hand side of (18) is not taken into account if (17) is simply evaluated at time-level n. Therefore, we propose to modify (17) such that the condition holds exact for the time-integration method under consideration.

6 FILTER

As mentioned in the previous section, for $k = k_\mathrm{c}$ the reduction factor $f(\widehat{G}_{k_\mathrm{c}}, \widehat{G}_p, \widehat{G}_q)$ should not be highly dependent on p and q. We discuss the construction of an appropriate filter accordingly, directly considering discrete physical space. For a symmetric filter, the associated transfer function is given by

$$\widehat{G}_k = c_0 + 2c_1\cos(kh) + 2c_2\cos(2kh) + \cdots, \tag{19}$$

where again h denotes the width of the computational grid, and $k_\mathrm{c} = \pi/h$. We impose $c_0 + 2(c_1 + c_2 + \cdots) = 1$ to get $\widehat{G}_0 = 1$. Note that for $0 \equiv c_2 \equiv c_3 \equiv \cdots$, the coefficients of the resulting 3-points filter are completely determined by the two conditions $\widehat{G}_{k_\mathrm{c}} = c_0 - 2c_1$ and $c_0 + 2c_1 = 1$. Then, it can be proven that the range of the function f for $k = k_\mathrm{c}$ is bounded by its value for the most local interaction (at $p = q = \frac{1}{2}k_\mathrm{c}$), and the most global interaction (at $q = 0$). To illustate the dependence on p and q, Figure 2 shows the range of $f(\widehat{G}_{k_\mathrm{c}}, \widehat{G}_p, \widehat{G}_q)$, as a function of $\widehat{G}_{k_\mathrm{c}}$. Note that for $\widehat{G}_{k_\mathrm{c}} = \frac{1}{2}$ the bandwidth of f is zero, implying that for this value of $\widehat{G}_{k_\mathrm{c}}$ there is no dependence of f on p and q.

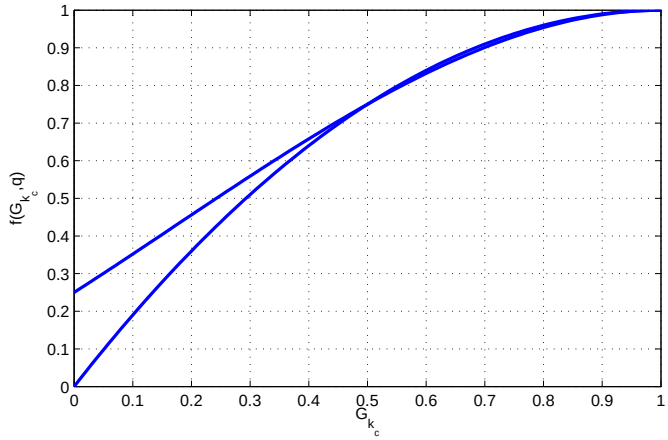

Figure 2: *Range of* $f(\widehat{G}_{k_\mathrm{c}}, \widehat{G}_p, \widehat{G}_q)$ *for a discrete 3-points filter, for* $0 \leq \widehat{G}_{k_\mathrm{c}} \leq 1$.

Figure 2 points out that for a 3-points filter, f has a substantial bandwidth, *i.e.* has a large dependence on p and q. In order to reduce the bandwidth of f, the stencil of the filter can be extended. Figure 3 shows how for a 5-points filter, the range of f is reduced using the obtained degree of freedom in c_2.

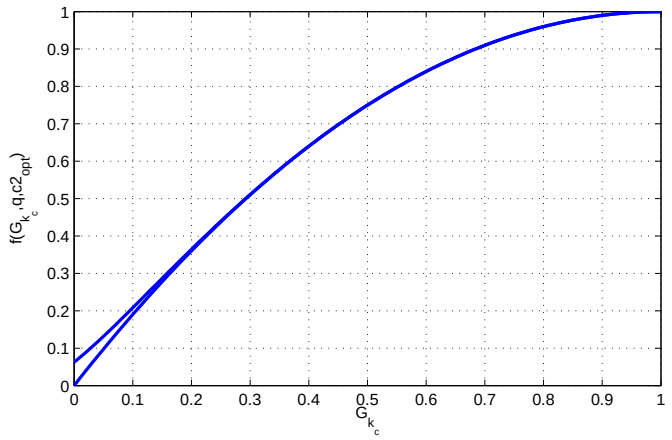

Figure 3: *Range of* $f(\widehat{G}_{k_c}, \widehat{G}_p, \widehat{G}_q)$*, for a discrete 5-points filter, for* $0 \leq \widehat{G}_{k_c} \leq 1$*. The degree of freedom in* c_2 *is used to minimize the bandwidth of* f*.*

7 RESULTS

The approximation $\mathcal{C}_4$ is used to solve the Burgers equation with Re $= 50$. As initial condition, $\hat{u}_k = k^{-1}$ has been taken. Since mode $k = 0$ has no interaction with other modes, we assume that $\hat{u}_0 = 0$, i.e. there is no mean flow. Figure 4 shows the energy spectrum of the steady state for $k_c = 20$, with and without the regularization method. A time step of $\delta t = 0.001$ has been used, and for the approximation method Eq. (17) has been modified using the time-discrete evolution given by (18). A DNS spectrum with $k_c = 100$ and $\delta t = 0.0005$ has been added as a reference. Clearly, for $k_c = 20$ the direct

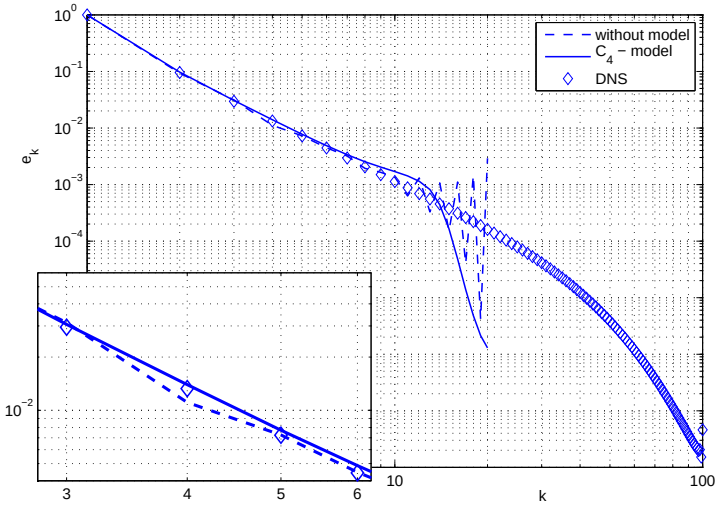

Figure 4: *Energy spectrum of the steady state solution of the Burgers equation, with and without the model, for* $k_c = 20$ *and* $\delta t = 0.001$*. The steady state was reached at* $t = 3$*, approximately.*

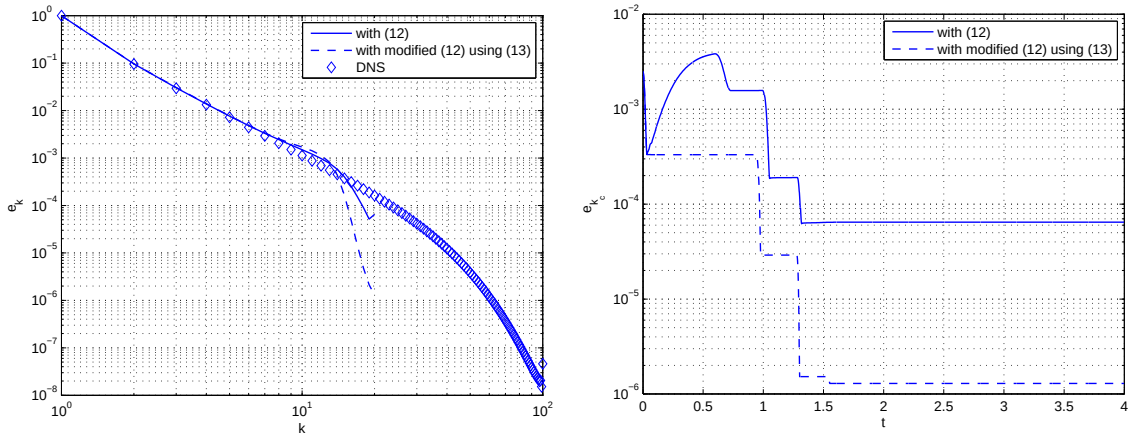

Figure 5: *Results using both the model with and the model without the last term in the right-hand side of* (18). *Left: as Fig. 4. Right: evolution of the energy at the highest wavenumber* e_{k_c}.

simulation without the model is not able to capture the physics correctly, as the energy is not dissipated enough at the high wavenumbers, and is reflected back towards the larger scales. The inset in Fig. 4 illustrates that the direct simulation with $k_c = 20$ is already a substantial amount off the reference DNS for $k = 4$. The regularization model shows a characteristic feature; due to energy conservation, the model compensates the energy loss at the smaller scales by an additional hump in the spectrum, just before the fall-off commences.

To investigate the influence of the last term in the right-hand side of (18), a simulation is done with and without this term, again for $k_c = 20$. Figure 5 shows the steady-state energy spectrum as well as the time evolution of the highest mode $\hat{u}_{k_c}$, for both simulations. Using (17) without taking the time-integration method into account, the energy at the highest mode is still able to grow; hence producing smaller scales of motion. With modification, i.e. when $\tilde{f}$ is evaluated according to (18), the energy is monotonically decreasing, and no modes smaller than $\hat{u}_{k_c}$ are produced. Furthermore, Fig. 5 illustrates that for most of the simulation time, the regularization model is turned on, corresponding with the horizontal sections in Fig. 5. Only for short periods of time the model is turned off, and energy is dissipated at the highest wavenumber.

Also the energy spectra for a range of values for k_c have been computed using the regularization method with time-discrete modification. Results for $k_c = 20, 30, 40, 50$ are shown in Fig. 6, again using a time step of $\delta t = 0.001$. For smaller values of k_c, the spectra at the high wavenumbers show an almost identical fall-off behavior, proportional to k^{-20}, approximately. This rapid fall-off is a desirable feature of the method, since it yields a small fall-off range of wavenumbers and hence the approximate solution is more likely to collapse with the DNS for a wider wavenumber range. For larger values of k_c, the tail of the spectrum shows a more moderate behavior, converging to the k^{-10} tail of the spectrum of the DNS. Also, Fig. 6 shows the number of modes that are still represented correctly

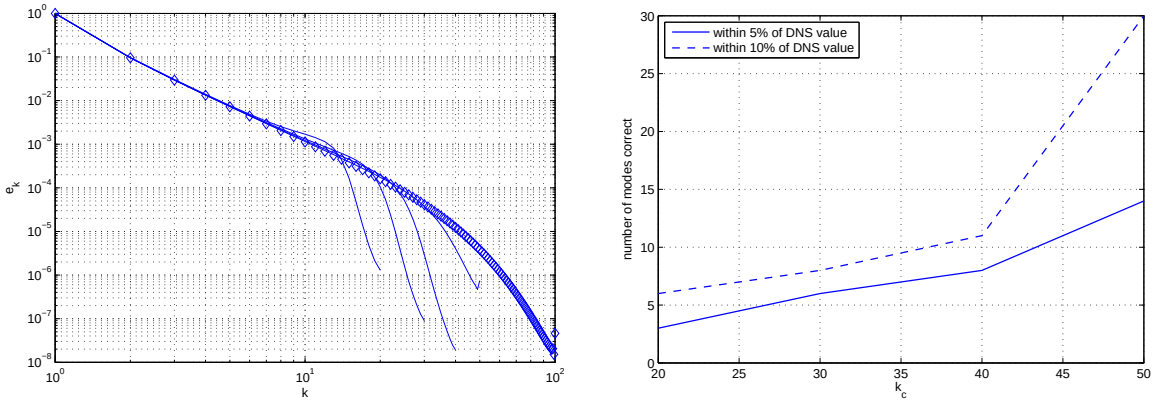

Figure 6: *Left: as Fig. 4, but now for* $k_c = 20, 30, 40, 50$. *Right: number of modes represented correctly by the model as a function of* k_c. *Both an error tolerance of* 5% *and* 10% *of the DNS are shown.*

by the model as a function of k_c. Both an error tolerance of 5% and 10% are shown. Note that the jump in the 10% tolerance at $k_c \approx 40$ is due to the fact that for larger values of k_c, the complete range of wavenumbers with an overshoot in the spectrum is within 10% of the DNS. For the 5% tolerance a similar jump has been observed at $k_c > 50$.

REFERENCES

[1] P.R. Spalart: Int. J. Heat and Fluid Flow **21**, 252 (2000)

[2] J.L. Guermond, J.T. Oden, S. Prudhomme: J. Math. Fluid Mech. **6**, 194 (2004)

[3] B.J. Geurts and D.D. Holm: Phys. Fluids **15**, L13 (2003)

[4] P. Sagaut: *Large Eddy Simulation for Incompressible Flows*, (Springer, Berlin 2001)

[5] J. Leray: Acta Math. **63**, 193 (1934)

[6] D.D. Holm, J.E. Marsden, T.S. Ratiu: Adv. Math. **37**, 1 (1998)

[7] C. Foias, O. Manley, R. Rosa, R. Temam: *Navier-Stokes equations and turbulence*, (Cambridge University Press, 2001)

[8] R. Verstappen: Comp. & Fluids, doi:10.1016/j.compfluid.2007.01.013 (available online 1 Oct. 2007).